

Hepatoprotective potential of four fruit extracts rich in different structural flavonoids against alcohol-induced liver injury via gut microbiota-liver axis

Yunyi Chen^a, Hanbing Ma^a, Jiaojiao Liang^a, Cui Sun^b, Dengliang Wang^c, Kang Chen^d, Jinmiao Zhao^d, Shiyu Ji^e, Chao Ma^f, Xianming Ye^g, Jinping Cao^a, Yue Wang^{a,*}, Chongde Sun^a

^a Laboratory of Fruit Quality Biology/The State Agriculture Ministry Laboratory of Horticultural Plant Growth, Development and Quality Improvement, Fruit Science Institute, College of Agriculture and Biotechnology, Zhejiang University, Hangzhou, China

^b Hainan Institute of Zhejiang University, Sanya, Hainan, People's Republic of China

^c Institute of Fruit Tree Research, Quzhou Academy of Agriculture and Forestry Science, Quzhou, China

^d Liandu Agriculture and Rural Bureau, Lishui, China

^e Lishui Agriculture and Rural Bureau, Zhejiang, China

^f Zhejiang NongZhen Food Co., Ltd., Hangzhou, China

^g Zhejiang JiaNong Fruit & Vegetable Co., Ltd., Quzhou, China

ARTICLE INFO

Keywords:

Fruits

Flavonoids

Alcoholic liver injury (ALI)

Oxidative stress

Ferroptosis

Gut microbiota

ABSTRACT

Alcoholic liver injury (ALI) accounts for a major share of the global burden of non-viral liver disease. In the absence of specialized medications, research on using fruit flavonoids as a treatment is gaining momentum. This study investigated the hepatoprotective effects of four fruits rich in structurally diverse flavonoids: oogan (*Citrus reticulata* cv. *Suavissima*, OG), mulberry (*Morus alba* L., MB), apple (*Malus × domestica* Borkh., AP), and turn-jujube (*Hovenia dulcis* Thunb., TJ). A total of one flavanone glycoside, three polymethoxyflavones, two anthocyanins, one flavonol glycoside, and one dihydroflavonol were identified through UPLC analysis. In an acute ethanol-induced ALI mouse model, C57BL/6J mice were supplemented with 200 mg/kg·BW/day of different fruit extracts for three weeks. Our results showed that the four extracts exhibited promising benefits in improving lipid metabolism disorders, iron overload, and oxidative stress. RT-PCR and Western blot tests suggested that the potential mechanism may partially be attributed to the activation of the NRF2-mediated antioxidant response and the inhibition of ferroptosis pathways. Furthermore, fruit extracts administration demonstrated a specific regulatory role in intestinal microecology, with increases in beneficial bacteria such as *Dubosia*, *Lactobacillus*, and *Bifidobacterium*. Spearman correlation analysis revealed strong links between intestinal flora, lipid metabolism, and iron homeostasis, implying that the fruit extracts mitigated ALI via the gut microbiota-liver axis. In vitro experiments reaffirmed the activity against ethanol-induced oxidative damage and highlighted the positive effects of flavonoid components. These findings endorse the prospective application of OG, MB, AP, and TJ as dietary supplements or novel treatments for ALI.

Abbreviations: ALI, Alcoholic liver injury; OG, Ougan; MB, mulberry; AP, apple; TJ, turnjujube; PMFs, polymethoxyflavones; NHP, neohesperidin; NOB, nobiletin; TAN, tangeretin; 5DN, 5-demethylnobiletin; C3G, cyanidin-3-O-glucoside; C3R, cyanidin-3-O-rutinoside; Q3G, quercetin-3-O-galactoside; DHM, dihydromyricetin; ALT, alanine aminotransferase; AST, aspartate aminotransferase; HDL-C, high-density lipoprotein cholesterol; LDL-C, low-density lipoprotein cholesterol; TC, total cholesterol; TG, triglycerides; Fe, total iron; MDA, malondialdehyde; GSH, glutathione; SOD, superoxide dismutase; CAT, catalase; GSH-Px, glutathione peroxidase; T-AOC, total antioxidant capacity; NRF2, nuclear factor erythroid-2-related factor 2; KEAP1, kelch-like ECH-associated protein 1; CUL3, cullin-3; HMOX1, heme oxygenase 1; NQO1, NAD(P)H-quinone oxidoreductase 1; GPX4, glutathione peroxidase 4; CHAC1, glutathione-specific gamma-glutamylcyclotransferase 1; ASCL4, acyl-CoA synthetase long-chain family member 4; FTH1, ferritin heavy chain 1; SLC7A11/xCT, Solute Carrier Family 7 Member 11.

* Corresponding author.

E-mail address: fruit@zju.edu.cn (Y. Wang).

<https://doi.org/10.1016/j.foodchem.2024.140460>

Received 16 March 2024; Received in revised form 24 June 2024; Accepted 12 July 2024

Available online 15 July 2024

0308-8146/© 2024 Elsevier Ltd. All rights are reserved, including those for text and data mining, AI training, and similar technologies.

1. Introduction

Latest research suggests that there is no safety threshold for alcohol consumption, with over 200 diseases or disabilities linked to drinking (Simon, Souza-Smith, & Molina, 2022) (Collaborators, 2018). Alcoholic liver injury (ALI), a nutritional disorder tied to hepatic metabolism, encompasses varying degrees of liver dysfunction caused by the direct or indirect effects of ongoing alcohol intake (Lucey, Im, Mellingen, Szabo, & Crabb, 2020). The prevalence of ALI has surged over the past decade, contributing substantially to the preventable liver-related morbidity and mortality worldwide, resulting in an enormous medical and economic burden (Jophlin et al., 2024).

A complicated and dynamic process underlies the onset and progression of ALI. Oxidative stress represents a principal trigger of physiological injury and pathological transformation of the liver, has occurred throughout ALI. Various sources of reactive oxygen species (ROS) interact with cellular components during ethanol metabolism, leading to lipid peroxidation, DNA mutation, and enzyme deactivation, culminating in hepatocyte injury (Yang, Cho, & Hwang, 2022). Abnormal fat accumulation, resulting from lipid transport and synthesis disorders, precipitates the development of fatty liver (Yan, Nie, Luo, Chen, & He, 2021). Attractively, ferroptosis, a newly discovered form of non-apoptotic cell death defined by iron-dependent, is deemed to be crucial to the advancement of liver disease (Chen, Li, Ge, Min, & Wang, 2022). The three foremost symptoms of ferroptosis are the imbalance of the SLC7A11/xCT-GSH-GPX4 axis, lipid peroxidation, and disrupted iron metabolism (Dixon et al., 2012). Despite the lack of precise mechanism on ferroptosis, lipid perturbation and iron overload are increasingly thought to be the universal traits of ALI (Wu & Meng, 2020). Moreover, there is a bidirectional communication between the gut with its microbiota and the liver via the bile ducts, portal vein, and systemic circulation, referred to as the “gut-liver axis” (Pabst et al., 2023). The gut microbiota, a key component of this axis, contributes to the progression of liver disease by impairing intestinal barrier integrity, distorting bile acid metabolism, and activating inflammatory responses (Hsu & Schnabl, 2023). Microbiome has emerged as an invaluable therapeutic target for alcohol-related liver diseases (Sarin, Pande, & Schnabl, 2019).

Biologically active secondary metabolites isolated from foodborne plants are more desirable in clinical practice than chemical drugs. A group of natural antioxidants known as flavonoids are particularly well regarded by researchers due to their broad distribution and minimal side effects. The tremendous diversity of flavonoids arises from the substitution of different sites and numbers of hydroxyl, methoxy, glycosides and other functional groups on the basic C6-C3-C6 skeleton (Wang et al., 2022). Existing studies claimed that there are several mechanisms involved in the biological processes of flavonoids against ALI, including activating ethanol dehydrogenase, regulating oxidative stress, hindering hepatic inflammation, improving lipid metabolism and preventing programmed cell death (Zhao et al., 2021) (Zhou et al., 2020) (Zhang et al., 2018) (Ma et al., 2023).

Fruits are an integral part of the human diet and a significant dietary source of flavonoids. Investigations has identified that ougan (*Citrus reticulata* cv. *Suavissima*, OG), mulberry (*Morus alba* L., MB), apple (*Malus × domestica* Borkh., AP) and turnujube (*Hovenia dulcis* Thunb., TJ) contain flavonoids with diverse structures as their active ingredients. The mature fruits of turnujube, especially the dried seeds, have long been applied in traditional remedies for alcohol detoxification and liver disease treatment in East Asia (Qiu et al., 2019). However, reports on the effects of the other three fruit varieties on ALI are scarce. The role of these four fruit extracts in counteracting alcohol-induced liver oxidative impairment, particularly in terms of ferroptosis inhibition and gut flora regulation, remains poorly understood. We hypothesized that these flavonoid-rich fruit extracts could defend against ALI by positively modifying the internal antioxidant status and remodeling the gut microbiota.

Therefore, this research was conducted with a bulk fruit (AP), two

“medicine food homology” fruits (MB, TJ) and a local specialty fruit in Zhejiang Province (OG). The representative flavonoids of these four fruit species were characterized, and their therapeutic potential against ALI was assessed multidimensionally through oxidative stress, lipid metabolism, ferroptosis, and intestinal microbiota using *in vitro* and *in vivo* models. This is the first study to compare the regulatory efficacy of natural products from different fruit sources on alcohol-induced “gut microbiota-liver axis” disorders.

2. Materials and methods

2.1. Preparation, identification and quantification of four fruit extracts

The fresh fruits at commercial maturity of OG, MB, AP and TJ were purchased from Lishui, Zhejiang, Shantou, Guangdong, Yantai, Shandong and Bozhou, Anhui, respectively. Fruits of relatively uniform size, free of mechanical or insect damage were selected as experimental materials. After washing, the peels of OG and the whole fruits of MB, AP, and TJ were fully freeze-dried in liquid nitrogen and ground into powder. The resulting powder was subsequently ultrasonically extracted with 95% ethanol (m: v = 1: 20) in three cycles and the supernatants were collected by centrifugation at 2655g for 8 min. The combined suspensions were filtered and vacuum dried with a rotary evaporator (Laborota 4000-efficient, Heidolph, Germany), and redissolved with purified water. Three-layer qualitative filter paper and 0.22 μm mixed cellulose esters membrane were then used for filtering, and the filtrates were lyophilized for 48 h using a vacuum freeze-dryer, yielding fruit extracts, which were stored at -20 °C for further experiment.

Determination of flavonoids with high performance liquid chromatography (HPLC) analysis was performed via Waters e2695 HPLC System specified with a Sunfire C18 ODS column (4.6 × 250 mm, 5 μm, Waters Corp., Milford, MA, USA) and a 2998 PDA Detector (Waters Corp., Milford, MA, USA). Gradient elution was selected during detection, the detailed analysis parameters, including gradient elution conditions for mobile phases A and B are provided in Appendix A.

Detected peaks were compared and identified with authentic standards: neohesperidin, nobiletin, tangeretin, 5-demethylnobiletin and dihydromyricetin were purchased from Shanghai Yuanye Biotechnology Co., Ltd. (Shanghai, China), cyanidin-3-O-glucoside, cyanidin-3-O-rutinoside and quercetin-3-O-galactoside were purchased from Sichuan Hengcheng Zhiyuan Biotechnology Co., Ltd. (Sichuan, China). For compound quantification, experiments were performed in triplicate and calculated via standard curve.

2.2. Animal experiment

Six- to eight-week-old male C57BL/6 J mice were obtained from Hangzhou Medical College. All the mice were housed in a controlled environment (20–24 °C, 40–70% relative humidity, 12-h light/dark cycle), and fed with a standard chow diet (Jiangsu Xietong Pharmaceutical Bioengineering Co., Ltd., Nanjing, China). The animal experiment design is depicted in Fig. 1B. Following a one-week acclimation period, the mice were randomly allocated into six groups (eight mice per group, four mice per cage), obtaining no statistical difference in initial body weight within each group. The specific groups comprised: a normal control group (CON), an alcohol model group (MOD), four groups for fruit extracts intervention (OG, MB, AP, TJ). The experiment consisted of two sessions: a dietary intervention stage and an acute alcohol-induced liver injury modeling stage. During the first two weeks, the fruit extracts intervention groups were administered corresponding fruit extracts at a dose of 200 mg/kg-BW/day, while the CON and MOD groups were fed with equal volume of distilled water. All fruit extracts were dissolved in distilled water. The acute alcohol-induced liver injury modeling was started in the third week. The CON group received daily oral doses of distilled water and the MOD group was given a gavage of 50% (v/v) ethanol solution at a dose of 12 mL/kg-BW/day, one hour

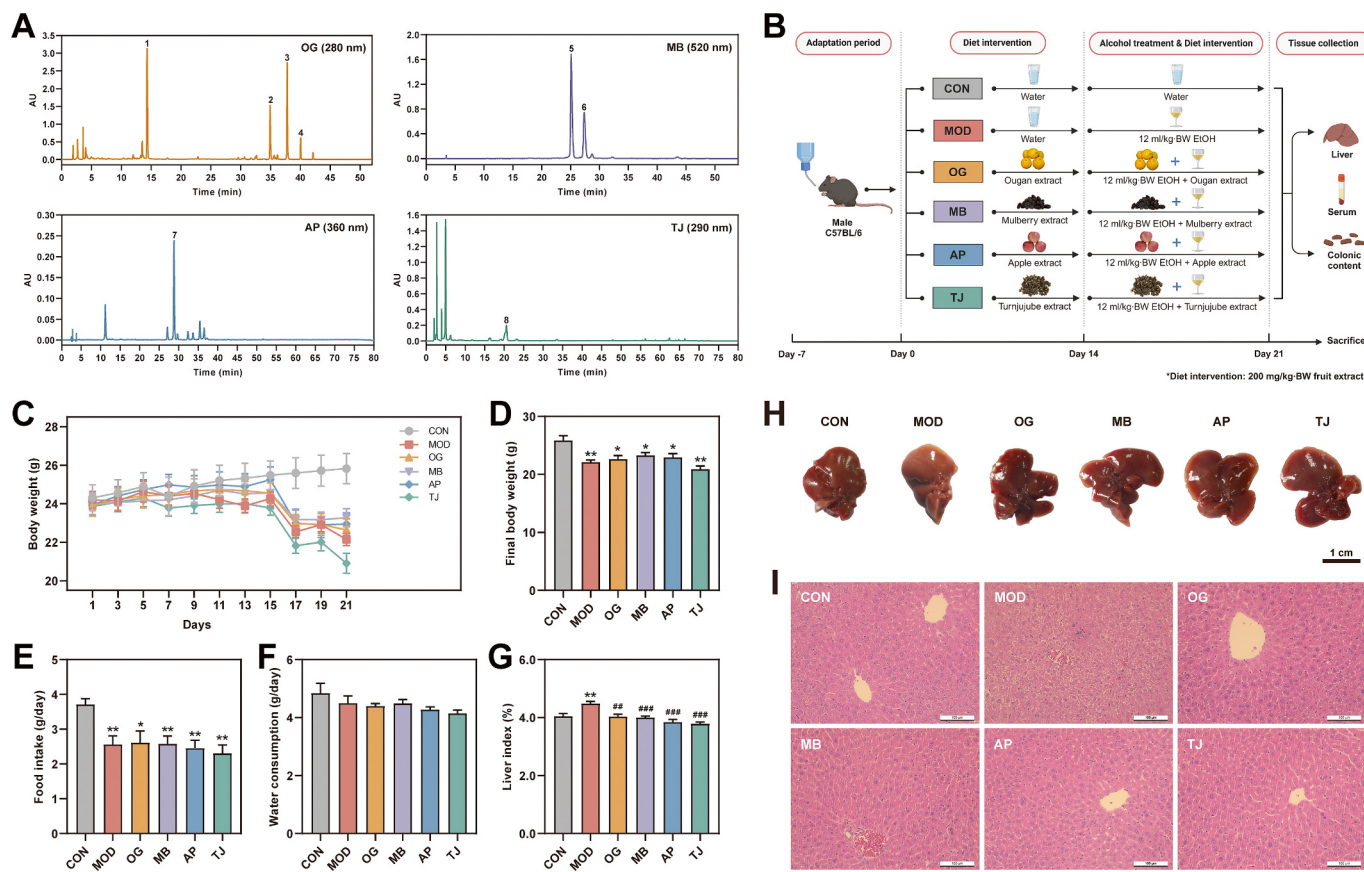


Fig. 1. OG, MB, AP, and TJ extracts alleviated alcohol-induced liver injury in mice. (A) HPLC chromatogram of four fruit extracts. Peak 1: NHP, peak 2: NOB, peak 3: TAN, peak 4: 5DN, peak 5: C3G, peak 6: C3R, peak 7: Q3G, peak 8: DHM. (B) Study design for animal experiment. (C) Body weight changes during animal experiment. (D) Final body weight. (E) Average daily food intake. (F) Average daily water consumption. (G) The weight coefficient of liver at the end of the experiment. (H) Representative photographs of the liver of each group (Scale bar, 1 cm). (I) Typical pictures of H&E-stained liver of each group (Scale bar, 100 µm). $n = 6\text{--}8/\text{group}$. * compared with CON group, $^* p < 0.05$, $^{**} p < 0.01$, $^{***} p < 0.001$. # compared with MOD group, $\# p < 0.05$, $\#\# p < 0.01$, $\#\#\# p < 0.001$.

after the oral delivery of distilled water. For the fruit extracts intervention groups, a dose of 200 mg/kg-BW/day of the respective fruit extracts was first administered, followed by a gavage of 50% (v/v) ethanol solution at a dose of 12 mL/kg-BW/day, one hour later. In the experiment, the body weight, food intake, and water consumption were recorded every 3 days. This animal experiment was undertaken with authorization from the Committee on the Ethics of Animal Experiments of Zhejiang University (ZJU20230200).

2.3. Euthanasia and biomaterial collection

The mice were euthanized by cervical dislocation at the end of the experimental period. Blood was collected by enucleation and centrifuged to obtain serum for biochemical analysis. Following an expedited laparotomy, the liver was carefully separated and weighed. Liver tissue from the same region of the right lobe was sliced and fixed in 4% paraformaldehyde (Beyotime Biotechnology, Shanghai, China) for histological evaluation. For ultrastructural analysis, 1 mm³ liver samples from both the CON and MOD groups were preserved in 2.5% glutaraldehyde (Solarbio, Beijing, China). The remaining liver tissue was divided into three equal sections to detect biochemical markers, gene expression, and protein expression. Colonic contents were collected and quickly frozen in liquid nitrogen along with the remaining liver tissue, and stored at -80 °C for further use.

2.4. Histological evaluation

The fixed samples were subjected to a series of operations such as

dehydration, transparent, paraffin embedding, sectioned (4 µm in thickness) and stained with hematoxylin and eosin (H&E). The prepared pathological sections were histologically characterized by light microscopy.

2.5. Transmission electron microscope (TEM) assay

The tissues preserved in glutaraldehyde were removed and underwent conventional dehydration, osmosis, embedding, sectioning, and double staining with uranium acetate and lead citrate. The specimens were then examined with the transmission electron microscope (H-7700, Hitachi, Japan) at 80 kV.

2.6. Biochemical analysis

Serum biochemical indicators including alanine aminotransferase (ALT), aspartate aminotransferase (AST), high-density lipoprotein cholesterol (HDL-C), low-density lipoprotein cholesterol (LDL-C), total cholesterol (TC) and triglycerides (TG), liver-related peroxidation markers including total iron (Fe), malondialdehyde (MDA), glutathione (GSH) as well as the activities of key antioxidant enzymes (SOD, CAT, GSH-Px), were quantified using commercially available assay kits (Nanjing Jiancheng Bio Co., Nanjing, China) and a microplate reader in accordance with the manufacturer's instructions.

2.7. Real time-PCR (RT-PCR)

Total RNA extraction of liver tissues was performed with a

commercial kit (Easy-do Biotechnology Co., Ltd., Hangzhou, China), followed by quality and concentration assessment using a NanoDrop (Thermo Fisher Scientific Inc.). Reverse transcription of the RNA was conducted with a commercial kit (Nanjing Vazyme Biotech Co., Ltd., Nanjing China). Quantitative real-time PCR was carried out on the CFX96 Touch Real-Time PCR Detection System (Bio-Rad Laboratories, Inc.) with a SYBR qPCR kit (Vazyme). The primer sequences of the target genes were listed in Table S1. The relative expression levels were calculated using the $2^{-\Delta\Delta CT}$ method with β -actin serving as the endogenous control.

2.8. Western blot assay

Western blot assay was conducted according to our previous study with some modification (Chen et al., 2023). NP-40 Lysis Buffer (Beyotime) containing 1 mM PMSF was used to homogenize liver samples from three mice in each group with a homogenizer (FastPrep-24 5G, MP Biomedicals, Irvine, California, USA), and supernatant was collected after centrifugation. The extracted proteins were quantified deploying a BCA assay kit (Beyotime). Equal amounts of protein (50 µg) were loaded into the sample wells of 4–20% SDS-PAGE gels (SurePAGE, Genscript Biotech Corporation, Nanjing, China) for electrophoretic separation and transferred onto PVDF membranes (0.45 µm, Thermo Fisher Scientific, 88,518). The membranes were blocked with 5% skimmed milk for 1 h before being probed with primary antibodies for 3 h and secondary antibodies for 2 h at room temperature. The antibodies used in this study are listed in Table S2. Finally, an ECL chemiluminescence kit (Servicebio, G2014) was utilized to detect protein signals through a ChemiDoc XRS+ System (Bio-Rad), and Image Lab (Bio-Rad, Version 3.0) semi-quantified the protein bands. For target proteins, their expression levels were normalized to β -ACTIN.

2.9. 16S rRNA gene sequencing and analysis

Total microbial genomic DNA was extracted from colonic contents with an E.Z.N.A. stool DNA Kit (Omega BioTek, Norcross, GA, USA). The quality of genomic DNA was detected by 1% agarose gel electrophoresis. Subsequently, the V3-V4 hypervariable region of the gene encoding for bacterial 16S rRNA were amplified using universal primer pairs 338F (5'-ACTCCTACGGGAGGCAGCAG-3') and 806R (5'-GGAC-TACHVGGGTWTCTAAT-3'). Following the PCR amplification, the purified amplicons were pooled in equimolar and paired-end sequenced on an Illumina MiSeq PE300 platform (Illumina, San Diego, CA, USA) according to the standard protocols by Majorbio Bio-Pharm Technology Co. Ltd. (Shanghai, China). Raw data were quality filtered with fastp (v0.19.6) and spliced with FLASH (v1.2.7) to obtain high-quality clean reads. To process the optimized data, DADA2/Deblur sequence denoising methods were selected, and Amplicon Sequence Variant (ASV) was used to represent sequence and abundance data. ASVs were taxonomically assigned using the Naive bayes consensus taxonomy classifier implemented in QIIME2 based on the SILVA 16S rRNA database (v138).

2.10. Cell culture and cell viability assay

In a humidified incubator (37 °C, 5% CO₂), AML-12 mouse liver cell line was cultivated in DMEM/F12 medium supplemented with 10% fetal bovine serum (FBS), 2% HEPES and 1% antibiotic-antifungal mixture (100 U/mL penicillin, 100 µg/mL streptomycin, 0.25 µg/mL amphotericin B). Cells were passaged when reaching the confluence of 80–90%. Cells in logarithmic growth phase were harvested and seeded in 96-well or 6-well plates at a suitable number per well. After incubated in serum-free DMEM/F12 medium for 12 h, the cells were treated with 200 mM ethanol to establish an alcohol-induced liver injury cell model. 25–800 µg/mL fruit extracts and 1.25–100 µM pure monomers were added at the same time and co-incubated for 24 h. Cell viability was assessed using a CCK-8 kit (Meilunbio, Dalian, China) following the

instruction manual. DMSO and silibinin were used as the negative and positive control respectively. Each experiment was conducted at least three times independently in triplicate.

2.11. Determination of cellular ROS content and biochemical markers

For cellular ROS level detection, the cells co-cultured with ethanol and various fruit extracts or pure compounds were gently washed twice with PBS, and a DCFH-DA fluorescent probe (Beyotime) was diluted in serum-free DMEM/F12 at a final concentration of 10 µM and incubated with cells for 30 min at 37 °C. After aspiration of DCFH-DA solution and washing three times to sufficiently remove excess probes, fluorescence intensity was measured with a microplate reader at 488 nm excitation and 525 nm emission. Each experiment was conducted independently three times. For biochemical assessments, supernatant and cell were collected for analysis to ALT, AST, SOD, MDA and total antioxidant capacity (T-AOC), which were performed using commercially available kits (Nanjing Jiancheng) following the guidelines.

2.12. Statistics

The statistical analysis was carried out with IBM SPSS Statistics software (version 26.0, IBM, Chicago, IL, USA). All data were expressed as mean ± standard error of the mean (SEM). The Mann-Whitney *U* test (for non-parametric data sets) or independent samples' Student's *t*-test (for parametric data sets) was used for two groups' comparison. And the one-way analysis of variance (ANOVA) with Tukey test was used for multi-group comparisons. *p* < 0.05 was considered statistically significant. Alpha diversity was calculated with Mothur-v1.30. Hierarchical clustering analysis and principal coordinate analysis (PCoA) were performed based on the unweighted UniFrac distance and bray-curtis dissimilarity, respectively. Significantly differentially abundant taxa between groups were identified by the linear discriminant analysis (LDA) effect size (LEfSe) with an LDA threshold of 3.0. Graphs were plotted by GraphPad Prism 8.0 (GraphPad Software, San Diego, CA, USA).

3. Results

3.1. Identification and quantification of characteristic components of four fruit extracts

HPLC was applied to identify the representative flavonoids in different kinds of fruit extracts. Based on comparisons of retention time and maximum absorption wavelength of standards, a total of eight flavonoid compounds were identified as major constituents, including one flavanone glycoside, three polymethoxyflavones (PMFs), two anthocyanins, one flavonol glycoside, and one dihydroflavonol (Fig. 1A, S1, and Table S3). Obviously, the flavonoid profile varied in kind and content with different fruit species. Flavanones and PMFs were the most abundant substances in the OG extract. The contents of neohesperidin (NHP), nobiletin (NOB), tangeretin (TAN), and 5-demethylnobiletin (5DN) were 28.22 ± 0.97 mg/g DW, 6.75 ± 0.50 mg/g DW, 14.77 ± 0.96 mg/g DW, and 4.54 ± 0.36 mg/g DW, respectively. MB extract was relatively rich in cyanidin-3-O-glucoside (C3G) and cyanidin-3-O-rutinoside (C3R), notably 19.22 ± 0.02 mg/g DW and 31.11 ± 0.60 mg/g DW. For AP extract and TJ extract, quercetin-3-O-galactoside (Q3G, 2.36 ± 0.12 mg/g DW) and dihydromyricetin (DHM, 1.96 ± 0.08 mg/g DW) were observed as the predominant flavonoid components.

3.2. In vivo evaluation of the protective effects of four fruit extracts in an alcoholic-liver-injured animal model

Using a mouse model of acute alcoholic liver injury and fruit extracts for dietary intervention, we carried out a three-week *in vivo* evaluation experiment to explore the preventive effects of four different flavonoid-

rich fruit extracts against alcohol-induced liver damage (Fig. 1B). The results showed that alcohol intake caused a sharp decrease in food intake and body weight of mice, while there were no significant differences in water consumption (Fig. 1C to F). To a certain degree, the intervention of fruit extracts (except the TJ group) could alleviate the body-weight loss of mice, although this difference did not reach significance. Compared to the MOD group, fruit extracts supplementation significantly decreased the liver index of mice (Fig. 1G), illustrating that dietary intervention may be helpful in keeping liver from pathological hypertrophy. The mice liver in the MOD group had an aberrant color and a loss of luster, as seen in Fig. 2H, whereas the livers in the other groups were a vivid red color. H&E staining additionally demonstrated that the alcohol administration could cause hepatocyte edema, sparse cytoplasm, and a tiny infiltration of inflammatory cells (Fig. 2I). On the contrary, hepatocytes treated with fruit extracts showed considerable improvements in their structural disorder, reflected by the reduction of vacuoles and the well-organized arrangement of hepatic cords, indicating a gratifying hepatoprotective effect. It is also noteworthy that TEM observation visualized the liver mitochondrial damage of mice in the MOD group (Fig. S2), including mitochondria shrunken, outer membrane rupture and reduction or even disappearance of internal cristae, in agreement with the typical features during ferroptosis reported previously (Li et al., 2020).

3.3. Four fruit extracts greatly benefited hepatic metabolism and antioxidant capacity in mice with alcoholic liver injury

Serum ALT and AST levels are sensitive indicators of liver injury. As could be seen from the test results of serum biomarkers (Fig. 2A), the enzyme level of mice in the MOD group was the most prominent among all groups. In contrast, the groups treated with fruit extracts before acute alcohol stimulation exhibited significant reduction. Overindulgence in alcohol often triggers lipid accumulation and metabolic dysfunction, marked by a notable rise in TC, TG, and LDL-C and a notable drop in serum HDL-C. All four types of fruit extracts were able to reverse these alterations to varying degrees, particularly the accumulation of TG.

Alcohol metabolism is known to be able to instigate oxidative stress via multiple approaches, with iron overload being one of the main variables that could facilitate ROS generation through the Fenton reaction. As shown in Fig. 2B, the liver iron content of alcohol-fed mice was dramatically greater than that of control-fed mice. The treatment of OG, MB, and AP extracts significantly reduced the level of hepatic iron, indicating that these three extracts may effectively alleviate alcohol-induced iron overload. To further analyze oxidative stress conditions, the MDA level and GSH content were measured, and we discovered increased lipid peroxidation along with a decreased antioxidant capacity under alcohol challenge. Pretreatment with OG, MB, and AP extracts effectively reversed the elevations in MDA levels compared to the MOD group. In the case of GSH level, only an improvement in the MB group showed significance. Concomitantly, fruit extracts also performed a vital function in attenuating the alcohol-induced suppression of key antioxidant enzyme activities (SOD, CAT, and GSH-Px). The above findings indicated the therapeutic potential of four types of fruit extracts in maintaining serum and liver metabolic equilibrium under alcohol-induced healthy stress.

3.4. Four fruit extracts activated NRF2-mediated antioxidant responses and ferroptosis resistance in mice with alcoholic liver injury

To investigate possible mechanisms of four kinds of fruit extracts against alcohol-induced liver injury, we first evaluated oxidative stress-related genes (*Nrf2*, *Keap1*, *Cul3*, *Hmox1*, *Nqo1*) and ferroptosis-related genes (*Gpx4*, *Chac1*, *Acls4*, *Fth1*) at the transcriptional level of liver tissue. RT-PCR analysis showed that alcohol stimulation significantly repressed the classical antioxidant pathway mediated by NRF2, as evidenced by the downregulation of *Nrf2* and upregulation of *Keap1* and

Cul3 (Fig. 2C). This trend was drastically reverted upon oral administration of the fruit extracts, with increased expression of the *Nrf2*-dependent antioxidative genes *Hmox1* and *Nqo1*. *Gpx4* and *Fth1* are negative regulators of ferroptosis, whereas *Chac1* and *Acls4* are positive regulators. All four fruit extracts greatly increased *Gpx4* expression and decreased *Acls4* expression compared to the model group. The expression of *Fth1* was considerably elevated upon intervention with OG, MB, and TJ extracts. But only the OG extract showed a pronounced reversal impact on the *Chac1* gene.

The expression levels of four key proteins were examined by Western blot assay. As shown in Fig. 2D and E, there were significant changes in the expression of ACSL4, NRF2, and xCT in liver tissue of alcohol-fed mice relative to the control group. Alcohol stimulation had the greatest impact on GPX4, with its expression level downregulated by 47.1%. Treatment with the fruit extracts reversed these markers, though the improvement effectiveness varied among the four exposure groups. Both the OG and AP groups enhanced NRF2, xCT, and GPX4 protein expression while decreasing ACSL4 protein expression, which was of statistical significance.

3.5. Four fruit extracts ameliorated gut microbiota dysbiosis in mice with alcoholic liver injury

In this study, the regulatory capability of four kinds of fruit extracts on intestinal microorganisms was investigated by 16sRNA sequencing. Alpha diversity was first analyzed and the results were shown in Fig. 3A. In the intestinal microbiota of alcohol-fed mice, the Chao and ACE indices reflecting community richness and the Shannon index reflecting community diversity showed a similar growing tendency, while the Simpson index (also indicating diversity) showed a visible decline. This demonstrated that short-term heavy drinking may impose the risk of over-proliferation of intestinal bacteria. However, no significant differences were observed between the fruit extract intervention groups and the model group except that the Simpson index was further decreased in the AP group. The results of the Beta diversity analysis, including hierarchical clustering analysis (Fig. 3B) and PCoA analysis (Fig. 3C), revealed that there were great differences in bacterial community structure at the ASV level between the MOD and CON group. Meanwhile, the species composition also changed noticeably after treatment with fruit extracts. Of these, the OG group and MB group tended to be close to the CON group along the PC2 axis, indicating that fruit extracts promoted a clear restructuring of intestinal microbiome in ethanol-fed model. The degree of bacterial taxonomic similarity at the phylum and genus level was then assessed to give a more comprehensive understanding on overall gut microbiota composition. At the phylum level (Fig. 3D), the predominant bacterial phyla were Firmicutes, Proteobacteria, and Actinobacteriota. Alcohol-feeding caused an overwhelming rise in the relative abundance of Firmicutes and a lower ratio of Firmicutes to Bacteroides compared to the CON group (Fig. S3A). The administration of fruit extracts partially reversed this trend, though the effect was not significant. At the genus level (Fig. 3E), a total of 23 genera (relative abundance >1%) were annotated and striking alterations in distribution proportion of dominant species were observed in different groups. Similarly, the Venn diagram (Fig. S3B, C) and the Circos map (Fig. S3D, E) also displayed the species distribution across various dimensions.

LEfSe analysis with a LDA threshold of 3.0 was performed to identify differentially abundant fecal bacteria. A total of 36 (compared with all groups) and 37 key discriminative genera (MOD vs. CON) were found (Fig. 4A and S3F). The first 15 genera with significant differences between each fruit extract treatment group and MOD group were selected, and the corresponding LDA values were shown in Fig. 4B. The microorganisms with the highest score in the OG, MB, AP, and TJ group were mainly *Allobaculum*, *Lactobacillus*, *Dubosiella*, and *Staphylococcus*. A detailed comparison of bacteria whose relative abundance ranked in the top 12 was shown in Fig. 4C. Particularly, there was an appreciable

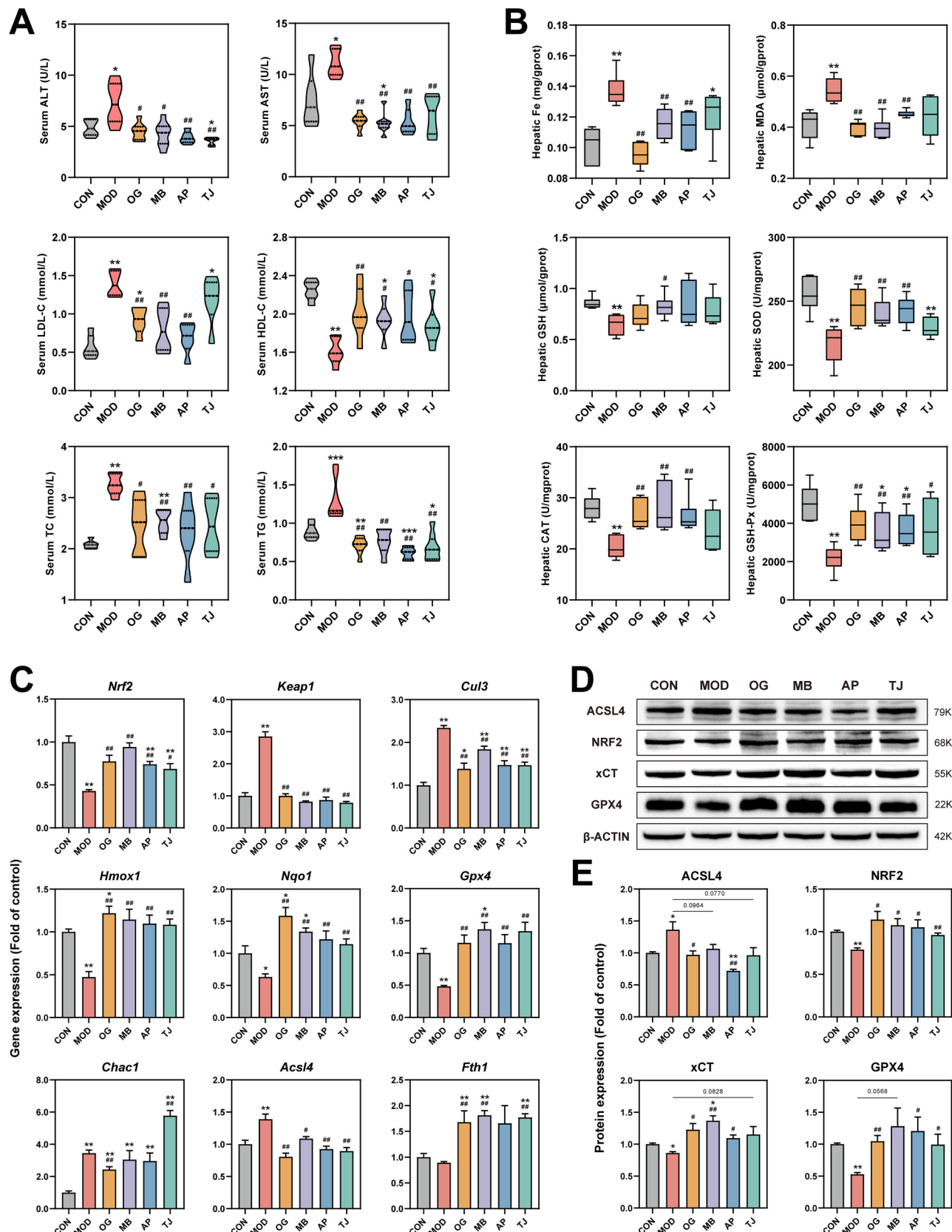


Fig. 2. OG, MB, AP, and TJ extracts maintained liver homeostasis by activating NRF2-mediated antioxidant responses and ferroptosis resistance. (A ~ B) Effects on serum and hepatic biochemical parameters ($n = 6\text{--}8/\text{group}$). (C) Gene expression profiles of liver tissue involved in oxidative stress and ferroptosis ($n = 6/\text{group}$). (B) Protein expression levels of hepatic ACSL4, NRF2, xCT and GPX4 semi-quantified by Western blot ($n = 3/\text{group}$). * $p < 0.05$, ** $p < 0.01$, *** $p < 0.001$. # compared with MOD group, ## $p < 0.05$, ## $p < 0.01$.

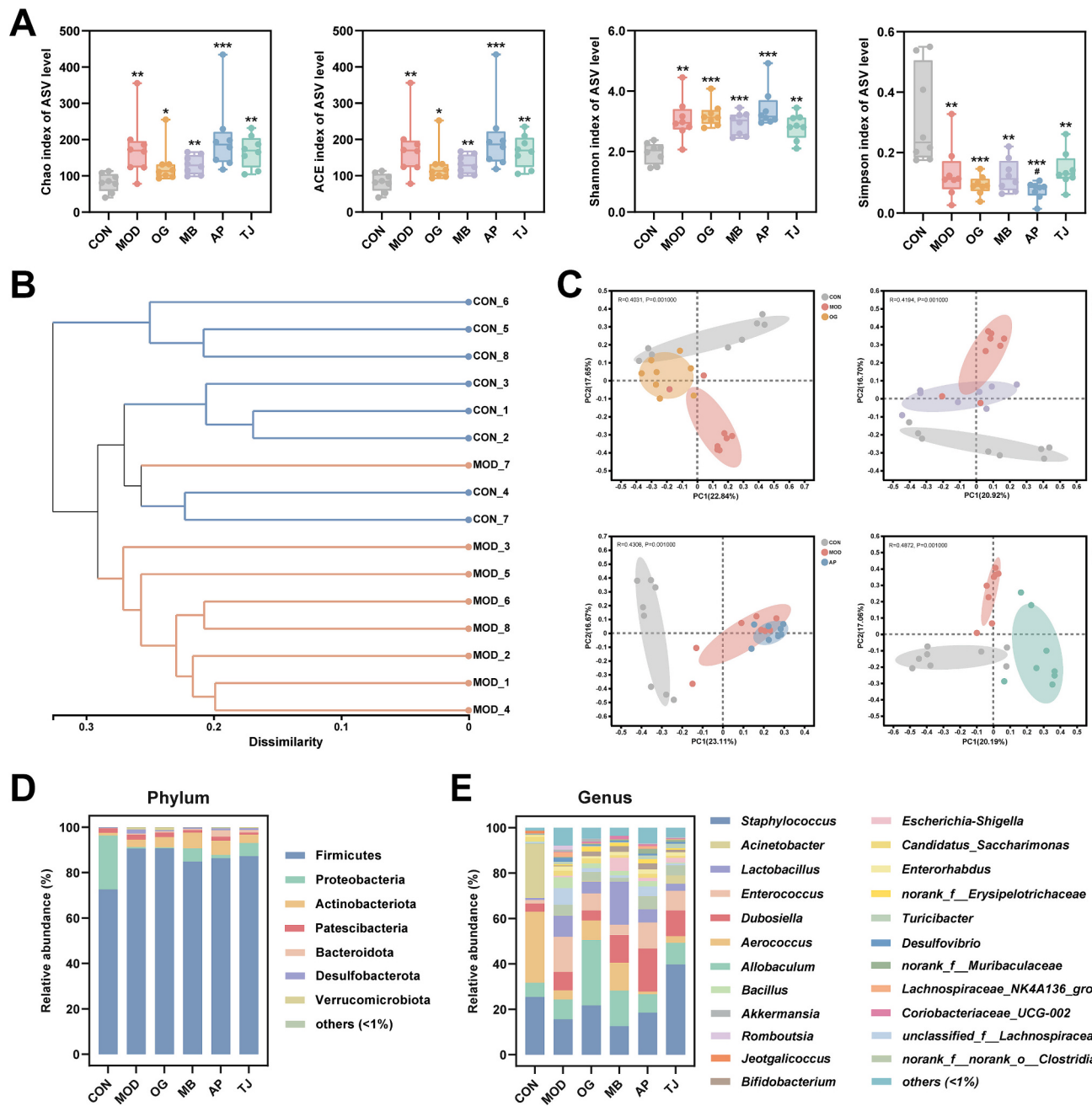


Fig. 3. Supplementation of four fruit extracts dramatically altered gut microbiota composition in mice with alcoholic liver injury. (A) Alpha diversity indices at the ASV level. Statistical significance was determined by the Mann-Whitney U test for two groups' comparisons. (B) Hierarchical clustering analysis at the ASV level. (C) PCoA plot of the gut microbiota composition at the ASV level. Difference analysis was performed by ANOSIM. The taxonomic composition distribution at the phylum level (D) and genus level (E) of gut bacteria. $n = 8/\text{group}$. * compared with CON group, * $p < 0.05$, ** $p < 0.01$, *** $p < 0.001$. # compared with MOD group, # $p < 0.05$.

down-regulation of *Enterococcus*, *unclassified_f_Lachnospiraceae*, and *Candidatus_Saccharimonas* in OG&MB groups, MB&TJ groups, MB&AP&TJ groups respectively, and an evident enrichment of *Bifidobacterium* in OG&MB&AP groups. In addition, we found that alcohol intake also facilitated the growth of *Akkermansia* and *Romboutsia*, whereas fruit extracts supplementation restored this imbalance and boosted the abundance of *Lactococcus* and *Faecalibaculum* (Fig. S3F).

Spearman correlation analysis was adopted to explore the association between intestinal flora structure and serum/liver biochemical indicators, seeking to uncover key species that contribute to hepatic damage (Fig. 4D). The results highlighted that the relative abundance of most bacterial genera had the highest correlations with serum lipid

levels and liver iron content. For example, *Enterococcus*, *unclassified_f_Lachnospiraceae*, *Escherichia-Shigella*, *Turicibacter*, *Romboutsia*, and *norank_f_Eubacterium_coprostanoligenes_group* were positively correlated with LDL-C, TC, and Fe levels ($P < 0.05$). *Dubosiella*, *Bifidobacterium*, *norank_f_Erysipelotrichaceae*, *Lactococcus*, and *Faecalibaculum* showed negative associations with TG level ($P < 0.05$). Other than this, PICRUSt2 functional prediction analysis based on MetaCyc and COG databases discovered a substantial alteration of alcohol stimulation on the functional structure of intestinal microorganisms, and the OG group shared the most similar functional characteristics with the CON group (Fig. S4). All the results above collectively prove that the ameliorative action of fruit extracts on ALI may be achieved by regulating the

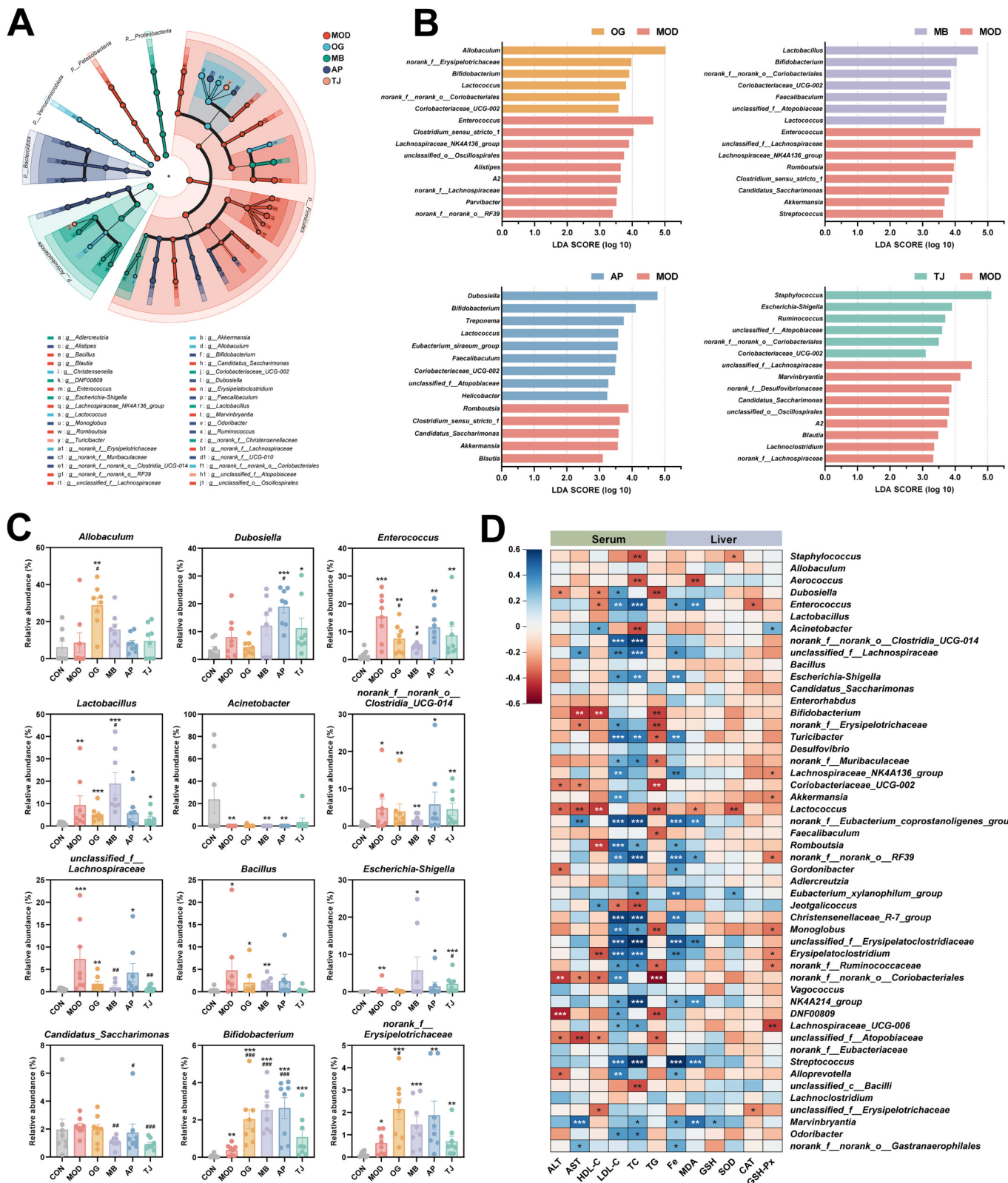


Fig. 4. Specific effects of four fruit extracts on the composition and abundance of microbial communities. (A) LEfSe analysis for differential abundant taxa detected among all groups. (B) LEfSe analysis between MOD group and each fruit extract group at the genus level. (C) Comparison of the top 12 discriminative genera. (D) Spearman correlation analysis between the discriminative genera and in vivo biochemical markers. n = 8/group. * compared with CON group, * p < 0.05, ** p < 0.01, *** p < 0.001. # compared with MOD group, # p < 0.05, ## p < 0.01, ### p < 0.001.

endogenous microflora configurations.

3.6. In vitro evaluation of fruit extracts and representative flavonoid monomers against oxidative stress in an ethanol-induced cell injury model

To further interrogate the biological efficacy of fruit extracts and individual flavonoid components, an *in vitro* injury model using the AML-12 cell line was established. The concentration of 25–100 µg/mL for extracts and 5 µM for monomers was employed given the outcomes of CCK-8 toxicity assessment (Fig. S5 and Table S3). As we can see in Fig. 5A, the cell viability and SOD activity decreased a great deal after being treated with ethanol for 24 h, and intracellular ROS and MDA accumulated in large quantities. Co-cultured with four fruit extracts greatly eliminated the deleterious influence of ethanol, showing a similar rescuing effect with positive control. Expectedly, eight flavonoid monomers could also diminish ethanol-induced viability declines and exhibited a stronger ROS scavenging capacity, yet no substantial variations were observed across different components (Fig. 5B). Ethanol exposure appeared to have a minor impact on T-AOC both in the supernatant and cells. Still, some monomers, such as NHP, 5DN, C3G, and C3R, were shown to considerably raise antioxidant capacity in cells and

their environment and might aid in oxidative damage resistance. As for the supernatant transaminase (ALT and AST) levels, OG extract and its primary ingredients, TAN and 5DN, exerted the most remarkable repression.

4. Discussion

Flavonoids, a diverse group of natural chemicals, exhibit numerous pharmacological effects in fruits. Flavonoids in fruits are specific to both variety and tissue. Previous studies have identified OG, MB, AP, and TJ as fruits rich in various structural types of flavonoids. In the present research, the representative compounds in fruit extracts were qualitatively and quantitatively analyzed by HPLC. Flavones and flavanones are most commonly observed in the *Citrus* genus. PMFs is a unique type of flavones in citrus fruits, which have more than two methoxy groups (-OCH₃) on their chemical skeleton (Saini et al., 2022). OG was identified as one of the varieties with the highest flavonoid content and the highest proportion of PMFs (Wang et al., 2017). Anthocyanins are key contributors to fruit coloration and putative health advantages of most berries. Consistent with previous results of UPLC-Triple-TOF/MS, MB fruit contained only two cyanidin derivatives (C3G and C3R), which

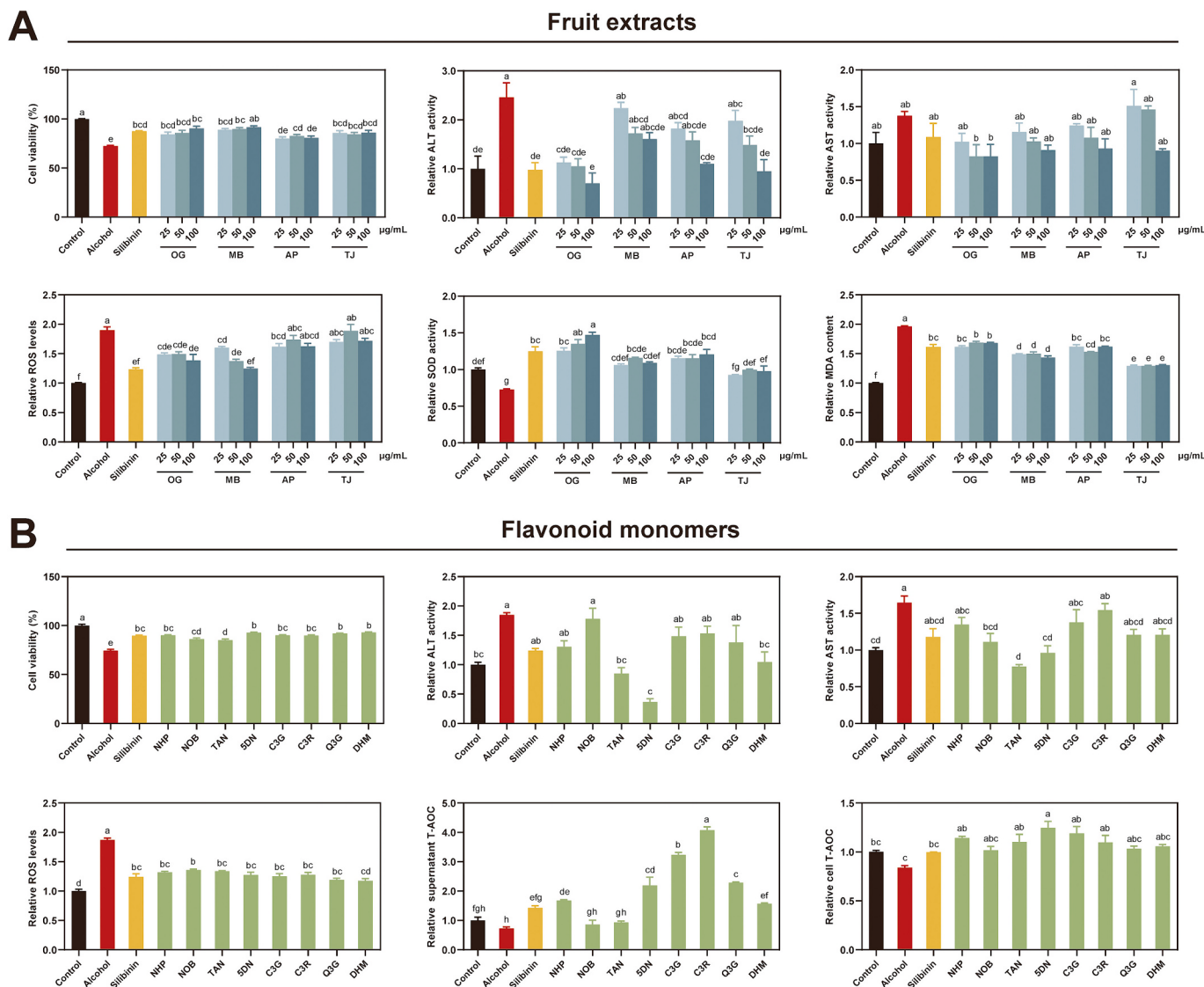


Fig. 5. The *in vitro* protective activity of four fruit extracts and representative flavonoid monomers against alcohol-induced oxidative damage. Effects of fruit extracts (A) and identified flavonoid compounds (B) on the cell viability, ALT, AST, ROS, SOD, MDA and T-AOC level of AML-12 cells after ethanol modeling. Cell assays were repeated three times independently. Columns with different letters indicate a significant difference at $p < 0.05$.

differed significantly from the anthocyanin profiles of blackberry, black goji berry, blueberry, red Chinese bayberry and raspberry (Chen et al., 2022). In a prior study, we determined the presence of 11 chief phenolic compounds in 35 different apple cultivars by HPLC and HRMS, classifying them into anthocyanins, phenolic acids, flavan-3-ols, flavonols, and dihydrochalcones, respectively (Liang et al., 2020). Flavonols, particularly quercetin glycosides, were the most prevalent flavonoids in AP. Under the present experimental conditions, the highest content of Q3G was noted in the apple extract among the flavonoid components. Regarding TJ fruits, relevant pharmacological studies have verified that flavonoids such as dihydromyricetin, dihydroquercetin and quercetin serve as the foundation for antialcohol and hepatoprotective activity, with DHM having a clear detoxifying effect (Qiu et al., 2019) (Chen et al., 2021a). In this work, the only flavonoid detected in the TJ extract was DHM, suggesting it may be the pivotal active ingredient.

Lipid accumulation in hepatocytes is the earliest sign of ALI (You & Arteel, 2019). There is a steady equilibrium between the catabolism and anabolism of fatty acids in the liver under normal physiological condition. Alcohol abuse disrupts this balance as ethanol-derived toxic metabolites profoundly affect multiple aspects of hepatic lipid metabolism, leading to the accumulation of lipid droplets, triglycerides, and cholesterol. Mechanistic studies have indicated that ethanol can enhance the activity of AMP-activated protein kinase (AMPK) and sterol-regulatory element binding proteins (SREBPs) related to adipogenesis, impair the signaling of peroxisome proliferator-activated receptor- α (PPAR- α), and inhibit fatty acid β oxidation, thereby altering lipid metabolism and causing hepatic steatosis (Jeon & Carr, 2020) (Hyun, Han, Lee, Yoon, & Jung, 2021). In the current research, a mouse model of acute alcoholic liver damage was successfully established. Sequential intervention of fruit extracts significantly reduced serum levels of LDL-C, TC and TG, and increase serum HDL-C, even though it fails to improve weight status and diet consumption. This suggests that all the four fruit extracts could correct the observed dyslipidemia by participating in triglycerides and cholesterol metabolic pathways.

Oxidative changes in the liver are recognized as a hallmark of ALI (Yang et al., 2022). Ethanol consumption induces the ROS formation through several pathways, mainly including the elevation of microsomal CYP2E1 activity, mitochondrial dysfunction, activation of innate immune response, and cytokine release. ROS generated through these processes further activate redox-sensitive proinflammatory signaling pathways, causing lipid peroxidation, protein denaturation and DNA adducts formation (Park, Lee, Sim, Seo, & Seo, 2022). Many organic compounds from natural sources including silymarin (Aghemo et al., 2022), resveratrol (Truong, Jun, & Jeong, 2018), and saponins (Bi et al., 2021), have been reported to reduce oxidative stress in the presence of hepatic injury. As shown by the results of the current study, four flavonoid-rich extracts and eight representative flavonoid monomers demonstrated outstanding antioxidant activities in the ALI model. These protective effects have been seen specifically in scavenging intracellular ROS, reducing the production of lipid peroxidation end products (MDA), and enhancing both enzymatic (SOD, CAT, GSH-Px) and non-enzymatic (GSH) antioxidant systems. Studies have identified the NRF2-KEAP1-CUL3 signaling pathway as a master regulator of the endogenous antioxidant response (Tu, Wang, Li, Liu, & Sha, 2019). Mechanistically, once dissociated from KEAP1, NRF2 translocates to the nucleus where it dimerizes with Hif-1 α/β and binds to antioxidant response elements (ARE) and hypoxia responsive elements (HRE), initiating the transcription of key detoxifying enzymes such as NQO1, HMOX-1, and GST, which protect cells against xenobiotic and oxidative stress (Tilg, Moschen, & Kaneider, 2011). According to RT-PCR and Western blot analysis, OG, MB, AP and TJ extracts were effective in modulating the gene and protein expression of NRF2 in mouse liver. All four fruit extract treatments promoted NRF2 dissociation and obstructed its ubiquitination degradation by down-regulating the expression of *Keap1* and *Cul3* genes. As such, these natural extracts may function as NRF2 activators to stimulate NRF2-dependent gene (*Hmox-1* and *Nqo1*) expression that

counteract oxidative stress.

Unlike well-known forms of cell death, ferroptosis is characterized by iron-dependent lipid peroxidation, which primarily manifests as changes in mitochondrial morphology at the subcellular level (Li, Cao, et al., 2020). The essence of this oxidative cell death is due to GPX4 inactivation and ROS production linked to iron ion-mediated Fenton reaction, which eventually leads to accumulation of damaging lipid peroxides (Tang, Chen, Kang, & Kroemer, 2021). Oxidative stress and iron accumulation are necessary for triggering ferroptosis. Liver is the main organ responsible for iron storage, suggesting the possible important role of ferroptosis in ALI. Several more recent studies have validated this correlation and revealed that over half of the ALI patients presented with iron deposition in the liver (Luo et al., 2023) (Jia et al., 2021). Here we show that total intracellular iron level remarkably increased in the liver of C57BL/6 J mice following alcohol gavage, and fruit extracts supplementation contributed to a positive effect on hepatic iron homeostasis, likely through metal-chelating activity and by upregulating the iron-binding capacity of the major cytoplasmic iron storage protein (FTH1). Ferroptosis is an aberrant metabolic process controlled by three intrinsic defense mechanisms: the cyst(e)ine/GSH/GPX4 axis, the GCH1/BH4/DHFR axis and the FSP1/CoQ10 axis (Zheng & Conrad, 2020). The cyst(e)ine/GSH/GPX4 axis is considered the predominant system against ferroptosis in mammals, with GPX4 identified as a central regulator (Ursini & Maiorino, 2020). In this system, the cysteine/glutamine transporter (xCT) imports cystine into cells, which is then reduced to cysteine for GSH synthesis. GPX4, with the assistance of GSH, converts H₂O₂ and lipid peroxides into water or non-toxic lipid alcohols, maintaining cellular redox homeostasis. Our results suggested that alcohol stimulation led to GSH depletion and significant downregulation of GPX4 at both gene and protein levels, while dietary intervention could be very helpful in the recovery of GPX4 and xCT activities. Alternatively, CHAC1 was reported to specifically decompose GSH and thought to be upregulated under ferroptotic conditions (Wang et al., 2023). A similar gene expression trend was observed in our ALI model, with OG and TJ extract showing drastically distinct regulatory effects. Besides, as one of the sensors of ferroptosis, ACSL4 is a crucial enzyme that oxidizes polyunsaturated fatty acids (PUFAs) to 5-hydroxyeicosatetraenoic acid (5-HETE) and generates lipid peroxides (Capelletti, Manceau, Puy, & Peoc'h, 2020). Fruit extracts treatments inhibited the expression of ACSL4 mRNA and protein in the livers of alcohol-fed mice to differing extents, especially at the gene level. These data open the possibility of fruit-derived natural products to protect against ferroptosis in ALI.

It is interesting to mention that growing evidence has identified NRF2 as a core element of ferroptosis regulation (Dang et al., 2022) (Anandhan et al., 2023) (Li et al., 2020), and its functions include: 1) targeting the GPX4 metabolic pathway and antioxidant enzymes such as HMOX-1 to exert an antioxidant role; 2) stabilizing iron metabolism by regulating iron storage and transport; and 3) blocking lipid peroxidation by directly affecting PPAR γ or indirectly affecting AMPK. Given the favorable biological effects of fruit extracts on NRF2, we speculate that OG, MB, AP, and TJ extracts may participate in NRF2-dependent cytoprotective responses. These responses include modulating antioxidant pathway (xCT, GPX4, HMOX-1, NQO1), iron metabolism pathway (FTH1), and lipid peroxidation pathway (ACSL4), thus countering alcohol-induced ferroptosis in hepatocytes.

The gut-liver axis is intricately linked to the pathophysiology of most liver disorders (Rodrigues, van der Merwe, Krag, & Wiest, 2024). The gut microbiota, acting as a source of diverse stimuli, generates bioactive metabolites from both endogenous (bile acids) and exogenous (diet and environmental) substrates (Park et al., 2022). These metabolites, such as short-chain fatty acids (SCFAs), can be transported to the liver via the portal vein, setting the stage for the gut-liver axis (Wiest, Albillios, Trauner, Bajaj, & Jalan, 2017). Researchers have observed the disruption of host-microbe interactions in several models of liver disease, including ALI (Albillios, de Gottardi, & Rescigno, 2020). Alcohol and its

metabolites alter the composition of gut microbes, weaken gut integrity and barrier function, and exacerbate enterogenic endotoxemia, a critical initial step in ALI development (Sarin et al., 2019). As described in our results section, there were significant abnormalities in terms of species, number, structure and function in the intestinal flora of alcohol-fed mice. Alcohol exposure resulted in the overgrowth of the majority of gut bacteria and a reduction in some beneficial bacteria, consistent with the recognized consequences of excessive alcohol consumption (Xu et al., 2022). Firmicutes, which contains a range of beneficial bacteria that prevent the invasion of opportunistic pathogens (Li et al., 2021), increased in relative abundance following alcohol consumption, while the potentially pro-inflammatory Proteobacteria decreased. This could be due to the pathogen defense mechanisms of the intestinal microbiome. Meanwhile, the F/B ratio, an indicator of gut health, significantly reduced in response to alcohol, which might lead to elevated serum LPS levels, corresponding with Duan et al. (Duan et al., 2024). Nutrition and dietary constituents are among the key factors influencing the structure and function of gastrointestinal microbial communities (Jardon, Canfora, Goossens, & Blaak, 2022). According to our results obtained here, supplemental intake of OG, MB, AP, and TJ extracts reversed alcohol-induced alterations in gut microbiota composition across various taxonomic levels, accompanied by greater relative abundance of *Allobaculum*, *Lactobacillus*, *Dubosiella* and *Staphylococcus*, respectively. The critical discriminative genera differed among the OG, MB, AP, and TJ groups, suggesting variations in the regulation manner of intestinal flora across the four fruit extracts, albeit with some intersections. Generally, fruit extracts pretreatment upregulated the community abundance of *Dubosiella*, *Lactobacillus*, *Bifidobacterium*, *norank_f_Erysipelotrichaceae*, *Faecalibaculum*, while perturbing the colonization of *Enterococcus*, *Romboutsia*, *unclassified_f_Lachnospiraceae*. These changes likely contribute to the maintenance of gut microbial homeostasis in alcohol-exposed mice, which in turn attenuates liver injury. Indeed, extensive research has been conducted on the curative potential of natural products as microecological modulators for ALI (Zhao et al., 2022). For instance, Li et al. discovered that the protective activity of polysaccharides from *Eucommia ulmoides* Oliv. leaves are ascribed to their anti-inflammatory, antioxidant, and prebiotic properties facilitated by the microbiota-gut-liver axis, manifesting in stabilized intestinal microecology, reduced intestinal hyperpermeability, and endotoxin infiltration (Li et al., 2024). Wang et al. also showed that natural polysaccharides could considerably restore the intestinal microbial composition in ALI mice and established a strong correlation between intestinal microorganisms and liver injury indicators (Wang et al., 2024). Similarly, we assessed the relationship between the discriminative genera at the genus level and biochemical parameters. Specific bacterial groups were highly correlated with serum and liver biomarkers, particularly lipid levels and iron content. This suggests that gut microbes associated with alcohol exposure could participate in regulating host lipid metabolism and iron homeostasis, though the precise mechanism requires further investigation.

Flavonoids are well documented for their hepatoprotective activity. A recent study indicated that NOB can activate the BMAL1-AKT-lipogenesis axis to counteract the adverse effects of an ethanol diet (Li et al., 2024). Its demethylated analog 5DN, however, appears to have superior anti-damage properties in our cell model, which aligns with previous structure-activity relationship studies (Wang et al., 2018; Zheng, Fang, Cao, Xiao, & He, 2013). C3G has been found to inhibit hepatic lipid accumulation and liver fibrosis, with an essential contribution coming from mitochondrial autophagy (He et al., 2024). Q3G exerts its regulatory effects on liver dysfunction in cell and animal models by enhancing antioxidant responses (Jang, 2022). The therapeutic properties of DHM on ALI, such as reversing alcohol intoxication, attenuating liver steatosis, and suppressing oxidative stress, are also well recognized (Chen et al., 2021b). In this work, in vitro experiments further validated the activity of the four fruit extracts in protecting hepatocytes from ethanol-induced oxidative damage and emphasized the

favorable effects of the identified flavonoid components. Hence, the health benefits of these fruit extracts might be largely attributable to their flavonoid content.

Overall, our findings pave the way for future translational studies. The identification of specific flavonoid profiles and their hepatoprotective effects can inform the development of targeted dietary supplements or pharmaceuticals. Understanding the modulation of the gut microbiota by these extracts also opens up new possibilities for gut health interventions. Nonetheless, the current work still has some limitations. Firstly, we should be aware of the complicated, dynamic, and context-dependent relationships that exist between the gut microbiota and the host. Broader investigations into intestinal barrier function, immunological aspects, metabolomes, and even the implementation of fecal microbiota transplantation trials are needed to explore the detailed mechanisms by which fruit flavonoids antagonize ALI. Secondly, evaluating the long-term efficacy and safety of the fruit extracts in a chronic alcohol consumption model will be imperative to determine whether these extracts provide sustained benefits.

5. Conclusions

In summary, our study identified the flavonoid profiles and evaluated the hepatoprotective capacities of four fruit extracts derived from OG, MB, AP, and TJ. Utilizing an acute ethanol-induced ALI mouse model, we observed several characteristic abnormalities associated with alcohol exposure, including an imbalance between antioxidants and oxidants, hepatic iron overload, lipid metabolism disorders, and gut microbiota dysbiosis. Supplementation with OG, MB, AP, and TJ extracts for three weeks significantly alleviated these adverse effects. The therapeutic potential is believed to be mediated by the modulation of the gut microbiota-liver axis, as evidenced by reductions in oxidative stress, ferroptosis, and lipid deposition, along with improvements in intestinal microecology (Fig. 6). Additionally, encouraging results from in vitro assays confirmed the protective ability of the fruit extracts and their major flavonoid components against ethanol-induced cell death and ROS accumulation in AML12 hepatocytes. This study delivers valuable insights into the health benefits of these fruits and underscores the application potential of natural flavonoid fractions in ameliorating alcohol-induced oxidative liver injury. Future research should prioritize unraveling the specific molecular pathways involved and evaluating the long-term safety and efficacy of these extracts across diverse populations.

CRediT authorship contribution statement

Yunyi Chen: Writing – original draft, Visualization, Validation, Methodology, Investigation, Formal analysis, Conceptualization. **Hanbing Ma:** Writing – original draft, Investigation. **Jiaoqiao Liang:** Methodology, Investigation. **Cui Sun:** Writing – review & editing, Validation, Funding acquisition. **Dengliang Wang:** Writing – review & editing, Resources. **Kang Chen:** Writing – review & editing, Resources. **Jinmiao Zhao:** Writing – review & editing, Resources. **Shiyu Ji:** Writing – review & editing, Resources. **Chao Ma:** Writing – review & editing, Resources. **Xianming Ye:** Writing – review & editing, Resources. **Jinping Cao:** Writing – review & editing, Validation, Funding acquisition. **Yue Wang:** Writing – review & editing, Supervision, Project administration, Funding acquisition, Conceptualization. **Chongde Sun:** Supervision, Project administration, Conceptualization.

Declaration of competing interest

The authors declare that they have no known competing financial interests or personal relationships that could have appeared to influence the work reported in this paper.

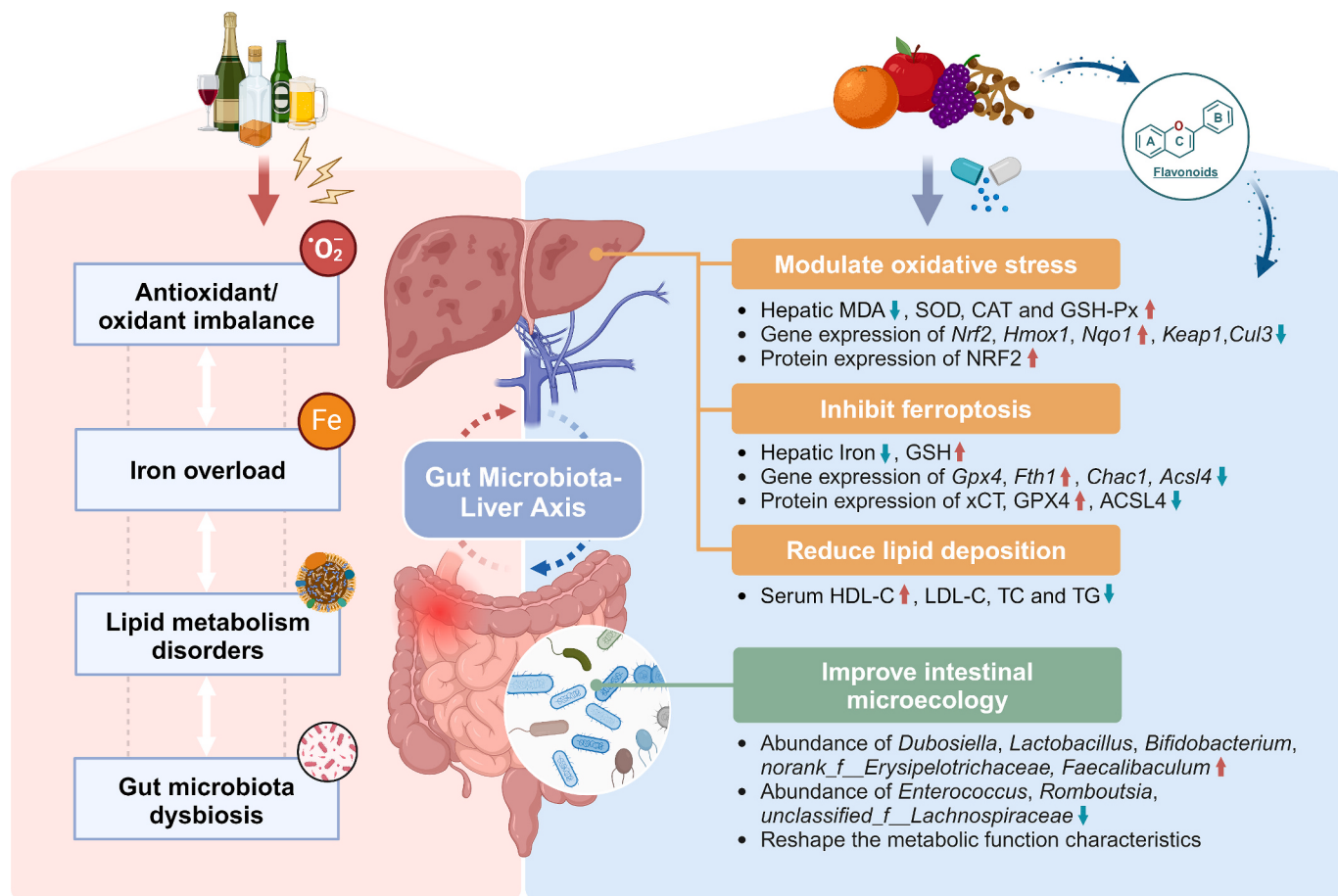


Fig. 6. Consumption of OG, MB, AP, and TJ extracts dramatically ameliorated alcoholic liver injury by targeting gut microbiota-liver axis. In hepatocytes, the intervention with these fruit extracts activated NRF2-dependent antioxidant responses and conferred resistance to ferroptosis, while also reducing lipid deposition. Simultaneously, the administration of fruit extracts significantly altered the gut microbiota composition and metabolic function, thereby improving intestinal microecology and further influencing host metabolism. Notably, flavonoid constituents appear to play vital roles in the observed hepatoprotective activity.

Data availability

Data will be made available on request.

Acknowledgements

This article was supported by Zhejiang Province Natural Science Foundation Joint Fund Project (LHZSD24C150001), the National Key Research and Development Program of China (2023YFD2300604), the National Natural Science Foundation of China (32101932, 32102021, 32072132), the Zhejiang Key R&D Development Project (2024C04030), the Fundamental Research Funds for the Central Universities (226-2022-00215), Quzhou characteristic citrus fruit quality detection project (2023-KYY-516103-0008), Ji'an Science and Technology Plan Project (20211-055350).

Appendix. Supplementary data

Supplementary data to this article can be found online at <https://doi.org/10.1016/j.foodchem.2024.140460>.

References

- Aghemo, A., Alekseeva, O. P., Angelico, F., Bakulin, I. G., Bakulina, N. V., Bordin, D., ... Yakovlev, A. A. (2022). Role of silymarin as antioxidant in clinical management of chronic liver diseases: A narrative review. *Annals of Medicine*, 54(1), 1548–1560. <https://doi.org/10.1080/07853890.2022.2069854>
- Albillios, A., de Gottardi, A., & Rescigno, M. (2020). The gut-liver axis in liver disease: Pathophysiological basis for therapy. *Journal of Hepatology*, 72(3), 558–577. <https://doi.org/10.1016/j.jhep.2019.10.003>
- Anandhan, A., Dodson, M., Shakya, A., Chen, J. J., Liu, P. F., Wei, Y. Y., ... Zhang, D. D. (2023). NRF2 controls iron homeostasis and ferroptosis through HERC2 and VAMP8. *Science Advances*, 9(5). <https://doi.org/10.1126/sciadv.ade9585>
- Bi, Y. F., Li, Q. Y., Tao, W. M., Tang, J. X., You, G. F., & Yu, L. (2021). Ginsenoside Rg1 and ginsenoside Rh1 prevent liver injury induced by acetaminophen in mice. *Journal of Food Biochemistry*, 45(8). <https://doi.org/10.1111/jfbc.13816>
- Capelletti, M. M., Manceau, H., Puy, H., & Peoc'h, K. (2020). Ferroptosis in liver diseases: An overview. *International Journal of Molecular Sciences*, 21(14). <https://doi.org/10.3390/ijms21144908>
- Chen, J., Li, X., Ge, C., Min, J., & Wang, F. (2022). The multifaceted role of ferroptosis in liver disease. *Cell Death and Differentiation*, 29(3), 467–480. <https://doi.org/10.1038/s41418-022-00941-0>
- Chen, J., Shu, Y., Chen, Y., Ge, Z., Zhang, C., Cao, J., ... Sun, C. (2022). Evaluation of antioxidant capacity and gut microbiota modulatory effects of different kinds of berries. *Antioxidants (Basel)*, 11(5). <https://doi.org/10.3390/antiox11051020>
- Chen, J., Wang, X., Xia, T., Bi, Y., Liu, B., Fu, J., & Zhu, R. (2021a). Molecular mechanisms and therapeutic implications of dihydromyricetin in liver disease. *Biomedicine & Pharmacotherapy*, 142, Article 111927. <https://doi.org/10.1016/j.bioph.2021.111927>
- Chen, J. B., Liu, Y., Wang, H. X., Liang, X., Ji, S. Y., Wang, Y., ... Sun, C. D. (2023). Polymethoxyflavone-enriched fraction from Ougan (*Citrus reticulata* cv. *Suavissima*) attenuated diabetes and modulated gut microbiota in diabetic KK-ay mice. *Journal of Agricultural and Food Chemistry*, 71(18), 6944–6955. <https://doi.org/10.1021/acs.jafc.2c08607>
- Chen, J. N., Wang, X. T., Xia, T., Bi, Y. H., Liu, B., Fu, J. F., & Zhu, R. Z. (2021b). Molecular mechanisms and therapeutic implications of dihydromyricetin in liver disease. *Biomedicine & Pharmacotherapy*, 142. <https://doi.org/10.1016/j.bioph.2021.111927>
- Collaborators, G. B. D. A. (2018). Alcohol use and burden for 195 countries and territories, 1990–2016: A systematic analysis for the global burden of disease study 2016. *Lancet*, 392(10152), 1015–1035. [https://doi.org/10.1016/S0140-6736\(18\)31310-2](https://doi.org/10.1016/S0140-6736(18)31310-2)

- Dang, R. Z., Wang, M. Y., Li, X. H., Wang, H. Y., Liu, L. X., Wu, Q. Y., ... Xie, P. (2022). Edaravone ameliorates depressive and anxiety-like behaviors via Sirt1/Nrf2/HO-1/Gpx4 pathway. *Journal of Neuroinflammation*, 19(1). <https://doi.org/10.1186/s12974-022-02400-6>
- Dixon, S. J., Lemberg, K. M., Lamprecht, M. R., Skouta, R., Zaitsev, E. M., Gleason, C. E., ... Stockwell, B. R. (2012). Ferroptosis: An iron-dependent form of nonapoptotic cell death. *Cell*, 149(5), 1060–1072. <https://doi.org/10.1016/j.cell.2012.03.042>
- Duan, W. H., Zhou, L. X., Ren, Y. L., Liu, F., Xue, Y. Z., Wang, F. Z., ... Geng, Y. (2024). Lactic acid fermentation of goji berries (*Lycium barbarum*) prevents acute alcohol liver injury and modulates gut microbiota and metabolites in mice. *Food & Function*, 15(3), 1612–1626. <https://doi.org/10.1039/d3fo03324d>
- He, Q., Yin, Z., Chen, Y., Wu, Y., Pan, D., Cui, Y., ... Wang, S. (2024). Cyanidin-3-O-glucoside alleviates ethanol-induced liver injury by promoting mitophagy in a Gao-binge mouse model of alcohol-associated liver disease. *Biochimica et Biophysica Acta, Molecular Basis of Disease*, 1870(6), 167259. <https://doi.org/10.1016/j.bbadi.2024.167259>
- Hsu, C. L., & Schnabl, B. (2023). The gut-liver axis and gut microbiota in health and liver disease. *Nature Reviews Microbiology*, 21(11), 719–733. <https://doi.org/10.1038/s41579-023-00904-3>
- Hyun, J., Han, J., Lee, C., Yoon, M., & Jung, Y. (2021). Pathophysiological aspects of alcohol metabolism in the liver. *International Journal of Molecular Sciences*, 22(11). <https://doi.org/10.3390/ijms22115717>
- Jang, E. (2022). Hyperoside as a potential natural product targeting oxidative stress in liver diseases. *Antioxidants*, 11(8). <https://doi.org/10.3390/antiox11081437>
- Jardon, K. M., Canfora, E. E., Goossens, G. H., & Blaak, E. E. (2022). Dietary macronutrients and the gut microbiome: A precision nutrition approach to improve cardiometabolic health. *Gut*, 71(6), 1214–1226. <https://doi.org/10.1136/gutjnl-2020-323715>
- Jeon, S., & Carr, R. (2020). Alcohol effects on hepatic lipid metabolism. *Journal of Lipid Research*, 61(4), 470–479. <https://doi.org/10.1194/jlr.R119000547>
- Jia, M., Zhang, H. M., Qin, Q. H., Hou, Y., Zhang, X., Chen, D., ... Chen, Y. L. (2021). Ferroptosis as a new therapeutic opportunity for nonviral liver disease. *European Journal of Pharmacology*, 908. <https://doi.org/10.1016/j.ejphar.2021.174319>
- Jophlin, L. L., Singal, A. K., Battaller, R., Wong, R. J., Sauer, B. G., Terrault, N. A., & Shah, V. H. (2024). ACG clinical guideline: Alcohol-associated liver disease. *The American Journal of Gastroenterology*, 119(1), 30–54. <https://doi.org/10.14309/ajg.00000000000002572>
- Li, A. Y., Yang, Y., Qin, S. K., Lv, S. J., Jin, T. H., Li, K., ... Li, Y. Z. (2021). Microbiome analysis reveals gut microbiota alteration of early-weaned Yimeng black goats with the effect of milk replacer and age. *Microbial Cell Factories*, 20(1). <https://doi.org/10.1186/s12934-021-01568-5>
- Li, J., Cao, F., Yin, H. L., Huang, Z. J., Lin, Z. T., Mao, N., ... Wang, G. (2020). Ferroptosis: Past, present and future. *Cell Death & Disease*, 11(2). <https://doi.org/10.1038/s41419-020-2298-2>
- Li, L., Fu, J. Q., Liu, D., Sun, J., Hou, Y. Y., Chen, C. J., ... Pi, J. B. (2020). Hepatocyte-specific deficiency mitigates high-fat diet-induced hepatic steatosis: Involvement of reduced PPAR γ expression. *Redox Biology*, 30. <https://doi.org/10.1016/j.redox.2019.101412>
- Li, X., Zhuang, R., Zhang, K., Zhang, Y., Lu, Z., Wu, F., ... Zhang, B. (2024). Nobletin protects against alcoholic liver disease in mice via the BMAL1-AKT-lipogenesis pathway. *Molecular Nutrition & Food Research*, e2300833. <https://doi.org/10.1002/mnfr.202300833>
- Li, Y. Z., Wang, H. M., Leng, X. P., Gao, J. M., Li, C., & Huang, D. F. (2024). Polysaccharides from *Eucommia ulmoides* Oliv. Leaves alleviate acute alcoholic liver injury by modulating the microbiota-gut-liver axis in mice. *Foods*, 13(7). <https://doi.org/10.3390/foods13071089>
- Liang, X., Zhu, T., Yang, S., Li, X., Song, B., Wang, Y., ... Cao, J. (2020). Analysis of phenolic components and related biological activities of 35 apple (*Malus pumila* Mill.) Cultivars. *Molecules*, 25(18). <https://doi.org/10.3390/molecules25184153>
- Lucey, M. R., Im, G. Y., Mellinger, J. L., Szabo, G., & Crabb, D. W. (2020). Introducing the 2019 American Association for the Study of Liver Diseases guidance on alcohol-associated liver disease. *Liver Transplantation*, 26(1), 14–16. <https://doi.org/10.1002/ltx.25600>
- Luo, J., Song, G., Chen, N. N., Xie, M. Y., Niu, X., Zhou, S. Y., ... Yu, D. K. (2023). Ferroptosis contributes to ethanol-induced hepatic cell death via labile iron accumulation and GPx4 inactivation. *Cell Death Discovery*, 9(1). <https://doi.org/10.1038/s41420-023-01608-6>
- Ma, D. D., Wang, Z. Y., He, Z. Y., Wang, Z. J., Chen, Q. M., Qin, F., ... Chen, J. (2023). Pine pollen extract alleviates ethanol-induced oxidative stress and apoptosis in HepG2 cells via MAPK signaling. *Food and Chemical Toxicology*, 171. <https://doi.org/10.1016/j.fct.2022.113550>
- Pabst, O., Hornef, M. W., Schaaf, F. G., Cerovic, V., Clavel, T., & Bruns, T. (2023). Gut-liver axis: barriers and functional circuits. *Nature Reviews Gastroenterology & Hepatology*, 20(7), 447–461. <https://doi.org/10.1038/s41575-023-00771-6>
- Park, J. W., Kim, S. E., Lee, N. Y., Kim, J. H., Jung, J. H., Jang, M. K., ... Suk, K. T. (2022). Role of microbiota-derived metabolites in alcoholic and non-alcoholic fatty liver diseases. *International Journal of Molecular Sciences*, 23(1). <https://doi.org/10.3390/ijms23010426>
- Park, S. H., Lee, Y. S., Sim, J., Seo, S., & Seo, W. (2022). Alcoholic liver disease: A new insight into the pathogenesis of liver disease. *Archives of Pharmacal Research*, 45(7), 447–459. <https://doi.org/10.1007/s12272-022-01392-4>
- Qiu, P., Dong, Y., Zhu, T., Luo, Y. Y., Kang, X. J., Pang, M. X., ... Ge, W. H. (2019). *Semen hooveniae* extract ameliorates alcohol-induced chronic liver damage in rats via modulation of the abnormalities of gut-liver axis. *Phytomedicine*, 52, 40–50. <https://doi.org/10.1016/j.phymed.2018.09.209>
- Rodrigues, S. G., van der Merwe, S., Krag, A., & Wiest, R. (2024). Gut-liver axis: Pathophysiological concepts and medical perspective in chronic liver diseases. *Seminars in Immunology*, 71. <https://doi.org/10.1016/j.smim.2023.101859>
- Saini, R. K., Ranjit, A., Sharma, K., Prasad, P., Shang, X., Gowda, K. G. M., & Keum, Y. S. (2022). Bioactive compounds of Citrus fruits: A review of composition and health benefits of carotenoids, flavonoids, Limonoids, and terpenes. *Antioxidants (Basel)*, 11(2). <https://doi.org/10.3390/antiox11020239>
- Sarin, S. K., Pande, A., & Schnabl, B. (2019). Microbiome as a therapeutic target in alcohol-related liver disease. *Journal of Hepatology*, 70(2), 260–272. <https://doi.org/10.1016/j.jhep.2018.10.019>
- Simon, L., Souza-Smith, F. M., & Molina, P. E. (2022). Alcohol-associated tissue injury: Current views on pathophysiological mechanisms. *Annual Review of Physiology*, 84, 87–112. <https://doi.org/10.1146/annurev-physiol-060821-014008>
- Tang, D. L., Chen, X., Kang, R., & Kroemer, G. (2021). Ferroptosis: Molecular mechanisms and health implications. *Cell Research*, 31(2), 107–125. <https://doi.org/10.1038/s41422-020-00441-1>
- Tilg, H., Moschen, A. R., & Kaneider, N. C. (2011). Pathways of liver injury in alcoholic liver disease. *Journal of Hepatology*, 55(5), 1159–1161. <https://doi.org/10.1016/j.jhep.2011.05.015>
- Truong, V. L., Jun, M., & Jeong, W. S. (2018). Role of resveratrol in regulation of cellular defense systems against oxidative stress. *Biofactors*, 44(1), 36–49. <https://doi.org/10.1002/biof.1399>
- Tu, W. J., Wang, H., Li, S., Liu, Q., & Sha, H. (2019). The anti-inflammatory and antioxidant mechanisms of the Keap1/Nrf2/ARE signaling pathway in chronic diseases. *Aging & Disease*, 10(3), 637–651. <https://doi.org/10.14336/Ad.2018.0513>
- Ursini, F., & Maiorino, M. (2020). Lipid peroxidation and ferroptosis: The role of GSH and GPx4. *Free Radical Biology and Medicine*, 152, 175–185. <https://doi.org/10.1016/j.freeradbiomed.2020.02.027>
- Wang, H. C., Yan, J. J., Wang, K., Liu, Y., Liu, S., Wu, K., ... Wang, X. M. (2024). The gut-liver axis perspective: Exploring the protective potential of polysaccharides from *Cistanche deserticola* against alcoholic liver disease. *International Journal of Biological Macromolecules*, 256. <https://doi.org/10.1016/j.ijbiomac.2023.128394>
- Wang, M., Meng, D., Zhang, P., Wang, X., Du, G., Brennan, C., ... Zhao, H. (2018). Antioxidant protection of Nobletin, 5-Demethylnobletin, Tangeretin, and 5-Demethyltangeretin from Citrus Peel in *Saccharomyces cerevisiae*. *Journal of Agricultural and Food Chemistry*, 66(12), 3155–3160. <https://doi.org/10.1021/acs.jafc.8b00509>
- Wang, Y., Liu, X. J., Chen, J. B., Cao, J. P., Li, X., & Sun, C. D. (2022). Citrus flavonoids and their antioxidant evaluation. *Critical Reviews in Food Science and Nutrition*, 62(14), 3833–3854. <https://doi.org/10.1080/10408398.2020.1870035>
- Wang, Y., Niu, H. C., Li, L. Y., Han, J., Liu, Z. H., Chu, M., ... Zhao, J. (2023). Anti-CHAC1 exosomes for nose-to-brain delivery of miR-760-3p in cerebral ischemia/reperfusion injury mice inhibiting neuron ferroptosis. *Journal of Nanobiotechnology*, 21(1). <https://doi.org/10.1186/s12951-023-01862-x>
- Wang, Y., Qian, J., Cao, J., Wang, D., Liu, C., Yang, R., ... Sun, C. (2017). Antioxidant capacity, anticancer ability and flavonoids composition of 35 Citrus (Citrus reticulata Blanco) varieties. *Molecules*, 22(7). <https://doi.org/10.3390/molecules22071114>
- Wiest, R., Albillas, A., Trauner, M., Bajaj, J. S., & Jalan, R. (2017). Targeting the gut-liver axis in liver disease. *Journal of Hepatology*, 67(5), 1084–1103. <https://doi.org/10.1016/j.jhep.2017.05.007>
- Wu, J., & Meng, Q. H. (2020). Current understanding of the metabolism of micronutrients in chronic alcoholic liver disease. *World Journal of Gastroenterology*, 26(31), 4567–4578. <https://doi.org/10.3748/wjg.v26.i31.4567>
- Xu, L., Li, W., Chen, S. Y., Deng, X. W., Deng, W. F., Liu, G., ... Cao, Y. (2022). Oenothein B ameliorates hepatic injury in alcoholic liver disease mice by improving oxidative stress and inflammation and modulating the gut microbiota. *Frontiers in Nutrition*, 9. <https://doi.org/10.3389/fnut.2022.1053718>
- Yan, J., Nie, Y., Luo, M., Chen, Z., & He, B. (2021). Natural compounds: A potential treatment for alcoholic liver disease? *Frontiers in Pharmacology*, 12, Article 694475. <https://doi.org/10.3389/fphar.2021.694475>
- Yang, Y. M., Cho, Y. E., & Hwang, S. (2022). Crosstalk between oxidative stress and inflammatory liver injury in the pathogenesis of alcoholic liver disease. *International Journal of Molecular Sciences*, 23(2). <https://doi.org/10.3390/ijms23020774>
- You, M., & Arteel, G. E. (2019). Effect of ethanol on lipid metabolism. *Journal of Hepatology*, 70(2), 237–248. <https://doi.org/10.1016/j.jhep.2018.10.037>
- Zhang, Y., Jin, Q., Li, X., Jiang, M., Cui, B. W., Xia, K. L., ... Nan, J. X. (2018). Amelioration of alcoholic liver steatosis by Dihydroquercetin through the modulation of AMPK-dependent lipogenesis mediated by P2X7R-NLRP3-Inflammasome activation. *Journal of Agricultural and Food Chemistry*, 66(19), 4862–4871. <https://doi.org/10.1021/acs.jafc.8b00944>
- Zhao, L., Wang, S. X., Zhang, N. H., Zhou, J. X., Mehmood, A., Raka, R. N., ... Zhao, L. (2022). The beneficial effects of natural extracts and bioactive compounds on the gut-liver axis: A promising intervention for alcoholic liver disease. *Antioxidants*, 11(6). <https://doi.org/10.3390/antiox11062111>
- Zhao, X. T., Gong, L. H., Wang, C., Liu, M. C., Hu, N. H., Dai, X. Y., ... Li, Y. X. (2021). Quercetin mitigates ethanol-induced hepatic steatosis in zebrafish via P2X7R-mediated PI3K/Keap1/Nrf2 signaling pathway. *Journal of Ethnopharmacology*, 268. <https://doi.org/10.1016/j.jep.2020.113569>
- Zheng, J. K., Fang, X., Cao, Y., Xiao, H., & He, L. L. (2013). Monitoring the chemical production of Citrus-derived bioactive 5-Demethylnobletin using surface-enhanced Raman spectroscopy. *Journal of Agricultural and Food Chemistry*, 61(34), 8079–8083. <https://doi.org/10.1021/acs.jafc.14027475>
- Zheng, J. S., & Conrad, M. (2020). The metabolic underpinnings of Ferroptosis. *Cell Metabolism*, 32(6), 920–937. <https://doi.org/10.1016/j.cmet.2020.10.011>
- Zhou, Y. J., Wang, S. F., Wan, T., Huang, Y. L., Pang, N. Z., Jiang, X. Y., ... Yang, L. L. (2020). Cyanidin-3-O- β -glucoside inactivates NLRP3 inflammasome and alleviates

alcoholic steatohepatitis via SirT1/NF- κ B signaling pathway. *Free Radical Biology and Medicine*, 160, 334–341. <https://doi.org/10.1016/j.freeradbiomed.2020.08.006>